Finite element modeling and experimental study of oblique soccer ball bounce

Key Words: Finite Element, Soccer Ball, oblique bounce

ABSTRACT

In this article a finite element model is developed to study the oblique soccer ball bounce. A careful simulation of the interaction between the ball membrane and air pressure in the ball makes the model more realistic than analytical models, and helps to conduct an accurate study on the effect of different parameters on the ball bouncing. This finite element model includes surface-based fluid cavity to model the mechanical response between the ball carcass and the internal air of the ball. An experimental setup was devised to study the ball bounce at soccer game-relevant impact conditions. The ball speed, angle and spin were measured before and after the bounce, as well as the ball deformation and the forces during the impact. The finite element model has been validated with three different test data, and the results demonstrate that the performed finite element model can be a valuable tool in the study of ball bounce. After validation of the utilized finite element model, the effect of the friction coefficient on soccer ball bounce was studied numerically. Simulation results show that increasing the friction coefficient may result into reversal of the horizontal impact force.

1. Introduction

In the game of association football (soccer), as in many other ball sports, the bounce of the ball plays a major role in the ball–surface interaction and affects to a great extent the way the game is played. For a field player, the ball bounce influences the correct moment of interception of a pass and thus is crucial for controlling the ball, or even anticipating the action of the adversary. Furthermore it affects the speed of the game, as a field with a faster ball rebound allows a quicker style of passing and attacking. On the other hand, unexpected changes in

ball speed, direction or spin on an unfamiliar field or even irregularities in ball rebound due to the unevenness of the field can deceive players, lead to mistakes and result in a lower technical quality of the game. This is especially the case for goal keepers, who are often confronted several times per game with shots on goal that are bouncing before they reach the goal. A miscalculation of the rebound behavior of the ball, whilst the goal keeper is diving for example, could result in a goal for the opposing team.

The governing bodies like Fédération Internationale de Football Association (FIFA) and Union of European Football Associations (UEFA) in football, or International Tennis Federation (ITF) in tennis, know the importance of the ball bounce and have therefore established requirements for fields for both vertical and oblique ball bounce, that are mandatory for football and recommended for tennis (FIFA, 2008a; ITF, 2009). The bounce behavior of the balls themselves is also controlled by governing body standards. The vertical ball rebound test aims at determining the rebound height of a ball when dropped on a rigid surface from a set height. In real game situations however, the ball will impact often at oblique angles. For this reason, the focus of this paper will be on oblique ball impact.

The (oblique) ball bounce behavior for a wide range of sports has also been the subject of numerous studies. Goodwill & Haake (2004) have studied the oblique impact of tennis ball with a tennis racket, and the generated ball spin. Haake, Carré, Kirk & Goodwill (2005) have modeled the oblique impact of a tennis ball on a surface and validated it with experimental data on a smooth (coefficient of friction of 0.51) and a rough (coefficient of friction of 0.62) surface. Their model combines the viscoelastic model, with the force of momentum-flux type model for

a normal impact, to oblique impact. This is a very interesting mathematical model for oblique tennis ball bounce which takes into account the fact that the normal reaction force may not act through the center of mass of the sphere and that the friction force may change direction during the impact. However their model does not contain the local deformations of the ball and uses an effective radius to determine the center of the mass of the ball during the impact.

Cross (2002a) has studied the grip-slip behavior of a bouncing ball by measuring the normal reaction force and the friction force during oblique impact of tennis balls, superballs, baseballs, basketballs and golf balls. Cross suggests that the bottom of the pressurized ball grips the surface and vibrates tangentially. His analytical model does not consider the interaction of the ball carcass and internal air of the ball.

In addition to this, Cross (2002b) has measured the horizontal coefficient of restitution for superballs and tennis balls. Penner (2002) and Arakawa et al. (2007) have done research on the ball bounce of golf balls. Penner has modeled the oblique impact of golf balls on a compliant surface using rigid ball theory. Arakawa et al. have investigated the effect of varying friction between the golf ball and smooth surfaces experimentally. Hubbard and Stronge (2001) have studied the bounce of table tennis balls. They have considered the table tennis ball as a thin-walled elastic shell, calculated the deformation and consequent contact forces and compared the results with both a finite element analysis and experimental data. Hamilton and Reinschmidt (1997) and Brancazio (1981) have modelled the bounce of a basketball on the backboard based on an analytical model that considers the ball as a solid sphere. As for football, Johnson, Reid &

Trembaczowski-Ryder (1972) and Percival (1976) have studied the normal impact and rebound of a football experimentally and numerically, using a momentum-flux model.

Besides the study of ball bounce, some researchers have studied soccer ball kicking. For example, Asai, Carre, Akatsuka, and Haake (2002) have studied the curve kick of the football. They have modeled the ball kicking leg and the surface of the ball by Lagrangian frame of reference and finite element method, and the air inside the ball with Eulerian frame of reference and finite volume method. Their model shows a very good potential to be applied for pressurized ball bounce studies.

Studies of the oblique bounce of a football however, have not yet been published to the best of our knowledge. Stronge and Ashcroft (2007) have modeled the oblique impact of inflated balls at large deflections (e.g. footballs), but no experimental data exist to evaluate their findings.

In summary, several theoretical models exist for the oblique ball bounce in different sports. They all try to predict the behavior of the ball after the bounce. However, none of these models have been evaluated with experimental data of footballs. The only experimental data for oblique football bounce are the test results from the accredited test houses that perform the standard FIFA test in order to approve a certain (artificial) field. Often these data are not published, and even if so, the problem remains that these tests only measure the horizontal speed before and after the ball bounce, and only at 13.9±1.4 m/s (50±5 km/h) at an angle of 15±2° to the horizontal. However, a fundamental measurement of all the relevant parameters of the oblique ball bounce (speed, angle and spin of the ball

before and after the bounce, as well as information on the ball forces and deformation) is not available.

Moreover, the influence of the surface on the oblique football bounce has not been studied yet. Whereas some studies have focused on influence of football properties (Price, Jones, & Harland, 2006b), little attention has been given to the influence of the surface on the way the ball bounces.

In this article a dynamic FE model of oblique soccer ball bounce was developed with ABAQUS Explicit software. The aim of this study was thus to develop a finite element model to simulate the oblique soccer ball bounce. This model will take into account the coefficient of friction (COF) between the ball and the surface, as well as the ball properties, and predict the ball rebound behavior in terms of speed, angle and spin. Ball bounce experiments using a high speed camera have been conducted to verify this model. The model can serve as a basis for a more extended model, where further material properties like damping and stiffness of the surface can be taken into account.

2. Experimental setup

The first goal of this study is to get an idea of realistic values for the ball bounce parameters. As mentioned earlier, in the standard FIFA test the ball is launched at 13.89±1.4 m/s (50±5 km/h) at an angle of 15±2° to the horizontal, without initial spin (FIFA, 2008b). However in a real game the ball will impact the pitch at a wide range of speeds, angles and spin rates. Speeds higher and lower than 13.89 m/s (50 km/h) will occur often, and the impact angle can be larger (e.g. the first bounce after a goal kick) or smaller (e.g. a hard pass or a bouncing shot on goal) than 15^{o}. Often the ball will strike the surface with a certain amount of spin. The

ball will get backspin for instance when it is chipped, or obtain topspin like in a half blocked or deflected shot.

In order to get an idea at which speed and under which angle a ball bounces onto the surface, two typical game situations are considered where the ball strikes the ground at high speed: a goal kick and a bouncing shot on goal. Lees and Nolan (1998) collated ball speed data from different studies of soccer kicks from experienced adult players. The maximum ball speed from each player was used to obtain a mean for each study in the range 20 to 30 m/s.

In this research an experimental setup for the oblique ball bounce test has been built. In order to launch the soccer balls in a reproducible way, a mechanical ball launching setup as illustrated in figure 1 was used. A Jugs ball pitching machine was adapted and mounted on a frame. By adjusting the sliding bar 1, the inbound angle α_i can be varied. The speed of wheels 2 and 3 define the launching speed v_i. By varying the speed of one of the wheels 2 or 3, top or backspin ω_i can be applied to the ball.

A high speed video camera (Photron ultima APX-RS) was used to film the experiments. A frame rate of 2000 frames per second (the exposure time of 1/2000 s) was used and the resolution was 640 by 320 pixels. A Matlab software tool has been developed in order to analyze the entire movement of the ball: ball speed, angle and spin before and after impact (Verhelst, R., Verleysen, P., Degrieck, J., Rambour S. & Schoukens, G., 2007). The tracking was automatic; the error on the position of the ball center was no more than 2 pixels.

Ball impact forces were measured using a Kistler force plate (model 9281 B11) installed under the surface operating at 5000 Hz and resonant frequency of 800 Hz

(resonant frequency of all principal directions equals 800 Hz). The measured force includes vertical and horizontal vectors which respectively correspond to normal and friction force.

3. Soccer ball

Before Adidas introduced the Roteiro ball made with thermal-bonding technology in 2004, a soccer ball was made of an assortment of manually stitched textile reinforced composite panels pressurized through an internal latex bladder (UEFA. 2004). A typical example of this is shown in figure 2. Now, more and more thermally-bonded balls like the Adidas Jabulani are used. In this study however, the modeling is based on the traditional balls.

The tensile response of the bladder and outer panel of this soccer ball are shown in figure 3. These diagrams have been extracted by Price, Jones, and Harland (2006a) from uniaxial tensile tests (The soccer ball in this experiment is very similar to the ball used in the reference). These properties are applied in the finite element model as hyperelastic materials with a Poisson's ratio of 0.490. To simplify the model, the stitched seam between the panels was not included. This simplification has no effect on the simulation of the impact parameters like coefficient of restitution and impact time. However, adding the stitched seam to the model will improve the accuracy of the deformation modeling by applying more realistic structural stiffness to the model (Price, Jones, & Harland, 2006a).

Moreover, in this study the gauge pressure of the ball is 1 bar (FIFA, 2007).

4. Finite element model

Considering the ratio of the ball wall thickness to its diameter, the carcass of the ball is simulated by composite shell elements, which include two inner (bladder)

and outer (outer panel) layers, with respectively 0.8 and 2.2 mm of thickness. 2400 quadrilateral shell elements are used to discretize the surface of the ball.

The deformation of the ball structure depends not only on the external loads like contact or kicking loads, but also depends on the pressure applied by the internal air. Pressure of the internal air in turn is affected by the deformation of the structure. Hence, in the dynamic simulation of the soccer ball, the modeling of the interaction between the ball carcass and the internal compressed air is the most critical item. The difficulty of the modeling is the coupling between the deformation of the structure and pressure exerted by the air.

In this simulation the feature surface-based fluid cavity is used to simulate the mechanical response between the ball carcass and the air. The cavity is assumed to be completely filled with the same properties and state. Fluid elements cover the surface of the solid material, and share the nodes of the surface of the solid body. Figure 4 shows an example of this combination. The nodes on the top surface of a shell element are used to create the surface-based fluid element.

The compressible fluid, air, is modeled as an ideal-gas with the following equation of state:

$$\tilde{P} = \rho R(\theta - \theta^Z) \qquad (1)$$

Where: $\tilde{P}$ is the absolute pressure (Pa), ρ is the fluid density at current pressure and temperature (kg/m^3), R is the gas constant (J/(K.mol)), θ is the current temperature (K), and θ^Z is the absolute zero temperature (K) (Yunus & Cengel, 2001).

The absolute pressure is the summation of the ambient pressure P_A and gauge pressure P

$$\tilde{P} = P + P_A \qquad (2)$$

A cavity reference node is associated with the fluid cavity. This node has a single degree of freedom representing the pressure inside the fluid cavity. It is also used in calculating the cavity volume. Indeed these hydrostatic fluid elements appear as surface elements that cover the cavity, but they are actually volume elements when the cavity reference node is accounted for. The dashed lines in figure 4 indicate that the element is actually pyramidal in shape (ABAQUS 6.9, 2010).

The surface-based fluid cavity capability can be used to model a liquid or gas-filled structure. It supersedes the element-based hydrostatic fluid cavity capability in functionality and does not require the definition of fluid elements.

While effects such as sloshing and wave propagation through the internal compressed air of the ball cannot be modeled with this method, the mechanical interaction between the internal air and ball carcass is simulated sufficiently.

Figure 5 depicts the finite element model of the impact of the soccer ball on the surface. In this method only the overall effect of the fluid inertia can be modeled; the constant pressure assumption in the cavity makes it impossible to model any pressure gradient-driven fluid motions. Thus, the approach assumes that the time scale of the excitation is very long compared to the typical response times for the fluid. However considering the ratio of the ball structure mass and the air inside the ball, this limitation is almost negligible in this study.

In the experiments a thin rubber mat of SBR (Styrene-Butadiene-Rubber) with the thickness of 7 mm was used on a rigid concrete surface. Based on experiments similar to the method presented by Cross (2002b) with a weight of 4 kg on the balls, the dynamic COF between the rubber mat and ball was 0.78, which was

applied in the simulation. The rubber mat was selected to have a uniform coefficient of friction over the entire contact surface, and was chosen to be thin enough not to affect substantially the coefficient of restitution (COF). Results of the drop test indicated that the effect of the rubber mat on the COR was less than 2 percent. Hence in this study for simplification the contacting surface was modeled as a rigid surface with the COF of 0.78. However the rigid surface can be easily replaced with a deformable surface if necessary in the model.

5. Results and discussion

This study includes two major objectives. The first objective is validation of the selected finite element model in the simulation of the oblique ball bounce. And the second objective is using this method to study the effect of the COF in soccer ball bounce.

The validation step contains three different cases. In the first case (case *I*) the soccer ball is launched obliquely with topspin rotation, and in the second case (case *II*) the soccer ball is launched obliquely with backspin rotation. In these two cases the impact velocity, impact rotation, impact angle, contact duration, rebound speed, rebound angle, and rebound rotation of the ball are measured. Then impact speed, impact rotation, and impact angle are implemented in the finite element model and output results are validated with the experimental measurements. In the third case (case *III*) the ball is launched without rotation. In this case the deformation of the ball is measured and compared with simulation measurements. Detail of each case is discussed in the following subsections.

5. 1. Case *I*. Ball is launched with initial topspin rotation

In the first case, the ball is launched with the initial topspin of about 59.66 rad/s, the impact speed of about 19.05 m/s, and the impact angle of about 29.60^{o} (the experiment was repeated four times and these quantities are the average of the five repetitions).

Applying those test inputs in the finite element model, results in very similar outputs of the ball impact. The high speed images and simulation results of the different stages of the ball impact are compared in figure 6. Some of the shell elements in the simulation are highlighted on the ball to make the rotation direction clearer. As seen in the images, the direction of the ball rotation before and after impact is topspin.

Figure 7 depicts the simulation results of the ball speed, angle, and rotation for the case *I*. Speed of the ball is 19.05 m/s before impact, then it slows down to 10m/s during impact, and increases again up to 15.60 m/s after impact. It is shown that the impact and rebound angles are respectively 29.60^{o} and 34.90^{o}. The impact rotational speed of the ball is -59.66 rad/s (negative spin corresponds to topspin rotation) and it rebounds with a spin of -101 rad/s.

In table 1 the simulation results are compared with the experimental measurements. As seen the experimental values for rebound speed, rebound angle, and rebound rotation of the ball are respectively 14.94 m/s, 33.60^{o}, and -100.48 rad/s. These results indicate that the simulation results correspond very well with experimental measurements.

In figure 8 the air pressure and the ball volume are represented. In the first 6 milliseconds after the inflation of the ball, the air pressure is stabilized on 1 bar. A

stiffness proportional damping has been applied to the material layers of the ball to model the viscoelastic behavior. Then during the impact it rises to 1.04 bar and decreases again to 1 bar after the ball bounce. Relatively, the volume of the ball decreases about 0.00012 m^3 during the impact period.

The experimental and simulation results of the normal and friction force are compared in figure 9. Once impact starts, the normal force increases and reaches a maximum of about 1500N after 4 milliseconds, and then it decreases to zero when the ball leaves the surface. The horizontal force shows a different behavior. When the contact starts, the horizontal force rises to almost 1000 N and its direction is opposed to the ball motion. Then it decreases to zero and is reversed. Both experimental and simulation results show that the horizontal force in this case reversed sign twice before it rebounds. The impact duration was about 8.5 milliseconds. The small phase divergence between the friction and normal force at the end of the impact can be due to the rubber mat. However, this effect is complex and not yet understood. It must be noted that the experimental data obtained from the force plate has not been filtered.

5. 2. Case *II*. Ball is launched with initial backspin rotation

In the second case, the ball is launched with the initial backspin of 58.40 rad/s, the impact speed of 18.08 m/s, and the angle of 22.90^o. The high speed images and simulation results of the ball bounce are compared in figure 10. As seen in the images, the direction of the ball rotation changes from backspin to topspin.

Figure 11 depicts the simulation results of the ball speed, angle, and rotation for case *II*. In this test, speed of the ball is 18.08 m/s before impact, then it decreases to 7 m/s during the impact time, and rebounds with 9.17 m/s. It is shown that the

impact and rebound angles are respectively 22.90 and 44.65^{o}. The impact rotational speed of the ball is 58.4 rad/s and it rebounds with the spin of -79 rad/s. Table 2 compares the simulation results with the experimental measurements.

The experimental values for rebound speed, rebound angle, and rebound rotation of the ball are respectively 9.22 m/s, 46.50^{o}, and -77.78 rad/s.

Like for case 1, in the first 6 milliseconds after the inflation of the ball the air pressure is stabilized on 1 bar (see figure 12). Then during the impact it increases to 1.03 bar and decreases again to 1 bar after the ball rebounds. Relatively, the volume of the ball decreases about 0.0001 m^3 during the impact period.

Figure 13 compares the simulation results and experimental measurements for normal and friction force in case *II*. It is shown that once impact starts, the normal force increases and reaches to its maximum of about 1150 N after 4.20 ms, and then it decreases back to zero when the ball leaves the surface.

In this case, the horizontal force is reversed at the end of the impact time. During the first 4.20 ms, the friction force increases up to about 1000 N while its direction is opposed to the ball motion, and then the friction force decreases and becomes zero 2.20 ms later.

So, after about 6.40 ms from the start of the impact, the friction force again goes up to 200 N, but its sign is reversed. Finally when the ball leaves the surface the friction force turns to zero. Like for the first case the impact duration is about 8 milliseconds.

5. 3. Case *III*. Deformation of ball

In the third step, the deformation of the ball is compared to the experimental results.

Figure 14 shows a typical deformation sequence. The deformation y is measured as the difference between the vertical position of the top of the ball and that same point for a ball that lies in rest on the surface (moment 0). The ball starts to make contact with the surface at moment 2, has maximum deformation at moment 3 and leaves the surface at moment 4.

The ball was launched with an impact angle of 25^{o} (relative to the horizontal direction) and with two different impact speeds of 19.44 and 25.00 m/s (70 and 90 km/h).

As seen in figure 15 experimental and numerical results correspond very well for both tests. On a rigid surface the ball deforms about 25 mm when it was launched with the speed of 19.44 m/s, while the deformation is about 30 mm for the impact speed of 25.00 m/s.

5. 4. Effect of the COF

In the fourth step, the effect of the COF on the ball bounce is investigated numerically. Models are made for an impact speed of 18.08 m/s, without rotation, impact angle of 22.90^{o} (similar to case *II*) and COF of 0.10, 0.30, 0.50, 0.60, 0.70, 0.80, and 0.90.

Figure 16, Figure 17, and Figure 18 represent the effect of the COF on the horizontal and vertical velocity, rebound angle, and rotation of the ball. As the COF increases from 0.10 to 0.60, the horizontal rebound velocity decreases from 15.89 m/s to 10.53 m/s, vertical rebound velocity does not change, the rebound angle rises up from about 24^{o} to 36^{o}, and the rotational velocity increases from about 18 rad/s to about 100 rad/s. By increasing the COF from 0.60 to 0.90, the

directions of variations change. The reason for this change can be found in the force curves.

The COF has almost no influence on the normal force (Figure 19), but affects the friction force considerably (Figure 20). For a COF below 0.60, the horizontal force is proportional to the normal force, suggesting that the ball is sliding throughout the bounce without changing the friction force direction. For a COF above 0.60, the frictional force drops to 0 after 4 to 5 ms (indicating that the ball is rolling at that point) and then even reverses sign (similar results are reported by Allen, Haake, & Goodwill (2010) for tennis ball bounce). This indicates that the ball is slipping or over-spinning, means that the horizontal velocity of the ball is smaller than the product of its radius and its angular velocity. As the friction at this point is no longer opposing the ball movement, an increase in horizontal velocity can be seen on Figure 16. The friction now works against the rolling of the ball (as it is slipping) and a reduction in ball spin can be seen in Figure 18. The higher the COF, the earlier the ball will start slipping in its contact phase. This explains why for the higher COF, the generated spin decreases and the rebound velocity increases: part of the rotational energy of the ball turns into translational energy.

6. CONCLUSION

Dynamic behavior of the oblique soccer ball bounce has been studied experimentally and numerically. Experimental studies have been performed with a setup which is devised to launch the soccer ball with flight conditions similar to those seen in a real game situation. Kinematics of the ball have been studied by

use of the high speed camera and the vertical and horizontal contact forces have been measured using a Kistler force plate installed under the surface.

A finite element model has been made to simulate the oblique ball bounce. In the dynamic simulation of soccer ball, surface-based fluid cavity elements have been used to simulate the mechanical response between the ball carcass and the internal air of the ball. Although effects such as sloshing and wave propagation through the fluid cannot be modeled with this method, results show that the mechanical interaction between the air and ball was simulated sufficiently.

Comparing the simulation and experimental results demonstrates that this model is very useful in the study of inflated ball impact. This ability can help to simulate the effect of the different parameters of the surface on the ball bounce. For example in this article the effect of the coefficient of friction on the oblique ball bounce has been studied. Results show that beyond a certain value of the friction coefficient the friction force sign changes and effects on the ball bouncing parameters.

By improving the model and applying more realistic material properties of a natural or artificial surface, it could be used to improve the construction requirements for these surfaces without the need for extensive experimental testing.

In the future, the model could be further extended for basketballs or other pressurized thin-walled spheres.

REFERENCES

ABAQUS 6.9 (2010), Theory manual, Hydrostatic fluid elements, section 3.8.

Allen, T., Haake, S., & Goodwill, S. (2010). Effect of friction on tennis ball impacts. Proceedings of the Institution of Mechanical Engineers Part P-Journal of Sports Engineering and Technology, 224(P3), 229-236.

Arakawa, K., Mada, T., Komatsu, H., Shimizu, T., Satou, M., Takehara, K., et al. (2007). Dynamic Contact Behavior of a Golf Ball during Oblique Impact: Effect of Friction between the Ball and Target. Experimental Mechanics, 47(2), 277-282.

Asai, T., Carre, M. J., Akatsuka, T., & Haake, S. J. (2002). The curve kick of a football I: impact with the foot. Sports engineering, 5, 183–192.

Brancazio, P. J. (1981). Physics of basketball. American journal of physics, 49(4), 356-365.

Cross, R. (2002a). Grip-slip behaviour of a bouncing ball. American journal of physics, 70 (11), 9.

Cross, R. (2002b). Measurements of the horizontal coefficient of restitution for a superball and a tennis ball. American journal of physics, 70(5), 482-489.

FIFA. (2007). FIFA Quality Concept for Footballs; The Test Criteria: Outdor Footballs. 2007 Edition. Retrieved from:

http://www.fifa.com/mm/document/afdeveloping/pitchequip/fqc_sales_doc_05_2007_13409.pdf

FIFA. (2008a). FIFA Quality Concept for Football Turf, Handbook of Requirements, 2008 Edition. Retrieved from:

http://www.fifa.com/mm/document/afdeveloping/pitchequip/fqc_requirements_manual_jan_2008_36016.pdf

FIFA. (2008b). FIFA Quality Concept for Football Turf, Handbook of Test Methods. 2008 Edition. Retrieved from:

http://www.fifa.com/mm/document/afdeveloping/pitchequip/fqc_test_method_manual_jan_2008_36019.pdf

Goodwill, S. R. & Haake, S. J. (2004). Ball spin generation for oblique impacts with a tennis racket. Experimental Mechanics, 44(2), 195-206.

Haake, S. J., Carre, M. J., Kirk, R. & Goodwill, S. R. (2005). Oblique impact of thick walled pressurized spheres as used in tennis. Proceedings of the Institution of Mechanical Engineers Part C-Journal of Mechanical Engineering Science, 219(11), 1179-1189.

Hamilton, G. R. & Reinschmidt, C. (1997). Optimal trajectory for the basketball free throw. Journal of Sports Sciences, 15(5), 491 - 504.

Hubbard, M. & Stronge, W. J. (2001). Bounce of hollow balls on flat surfaces. Sports Engineering, 4(2), 49-61.

ITF (2009). ITF Approved Tennis Balls & Classified Court Surfaces – a guide to products and test methods-January 2009 (online). Retrieved form:

http://www.itftennis.com/shared/medialibrary/pdf/original/IO_39369_original.PDF

Johnson, W., Reid, S. R. & Trembaczowski-Ryder, R. E. (1972). The impact, rebound and flight of a well inflated pellicle as exemplified in association football. Manchester Assoc. Eng, 5, 5.

Lees, A., & Nolan, L. (1998). The biomechanics of soccer: A review. Journal of Sports Sciences, 16(3), 211-234.

Penner, R. A. (2002). The run of a golf ball. Canadian Journal of Physics, 80, 931.

Percival, A. L. (1976). The impact and rebound of a football Manchester Assoc. Eng., 5, 11.

Price, D. S., Jones, R. & Harland, A. R. (2006a). Computational modelling of manually stitched soccer balls. Journal of Materials: Design and Applications, 220(4), 259-268.

Price, D. S., Jones, R. & Harland, A. R. (2006b). Soccer ball anisotropy modelling. Materials Science and Engineering A – Structural materials properties microstructures and processing, 420, 100-108.

Stronge, W. J. & Ashcroft, A. D. C. (2007). Oblique impact of inflated balls at large deflections. International Journal of Impact Engineering, 34(6), 1003-1019.

UEFA. (2004). Adidas matchballs, Retrieved on 1st January 2010 form:

http://www.uefa.com/uefachampionsleague/theball/

Verhelst, R., Verleysen, P., Degrieck, J., Rambour. & S, Schoukens, G. (2007). Development of a setup for the study of ball roll behaviour in soccer on artificial turf. Paper presented at the Science, Technology and research into sports surfaces-STARSS 2007.

Yunus, A. & Cengel, M. B. (2001). Thermodynamics: An Engineering Approach (4 ed.): McGraw-Hill.

Case *I*	Experiment	Standard deviation	Simulation	Agreement of the simulation with experiment
Impact speed	19.05 (m/s)	0.60 (m/s)	19.05 (m/s)	
Impact angle	29.60^{o}	0.67^{o}	29.60^{o}	
Impact rotation	-59.66 (rad/s) Topspin	2.72 (rad/s)	-59.66 (rad/s)	
Rebound speed	14.94 (m/s)	0.58 (m/s)	15.60 (m/s)	About 95%
Rebound angle	33.60^{o}	0.55^{o}	34.90^{o}	About 96%
Rebound rotation	-100.48 (rad/s) Topspin	1.25 (rad/s)	-101 (rad/s)	About 99%

Table 1: Comparison of the experimental results with simulation results for case *I*. (The experimental quantities are average of the five repetitions of the test)

Case *I*	Experiment	Standard deviation	Simulation	Agreement of the simulation with experiment
Impact speed	18.08 (m/s)	0.28 (m/s)	18.08 (m/s)	
Impact angle	22.90^{o}	0.81^{o}	22.9^{o}	
Impact rotation	58.40 (rad/s) Backspin	3.01 (rad/s)	58.40 (rad/s)	
Rebound speed	9.22 (m/s)	0.47 (m/s)	9.17 (m/s)	About 99 %
Rebound angle	46.50^{o}	0.78^{o}	44.65^{o}	About 96 %
Rebound rotation	-77.78 (rad/s) Topspin	1.17 (rad/s)	-79 (rad/s)	About 98 %

Table 2: Comparison of the experimental results with simulation results for case *II*. (The experimental quantities are average of the five repetitions of the test)

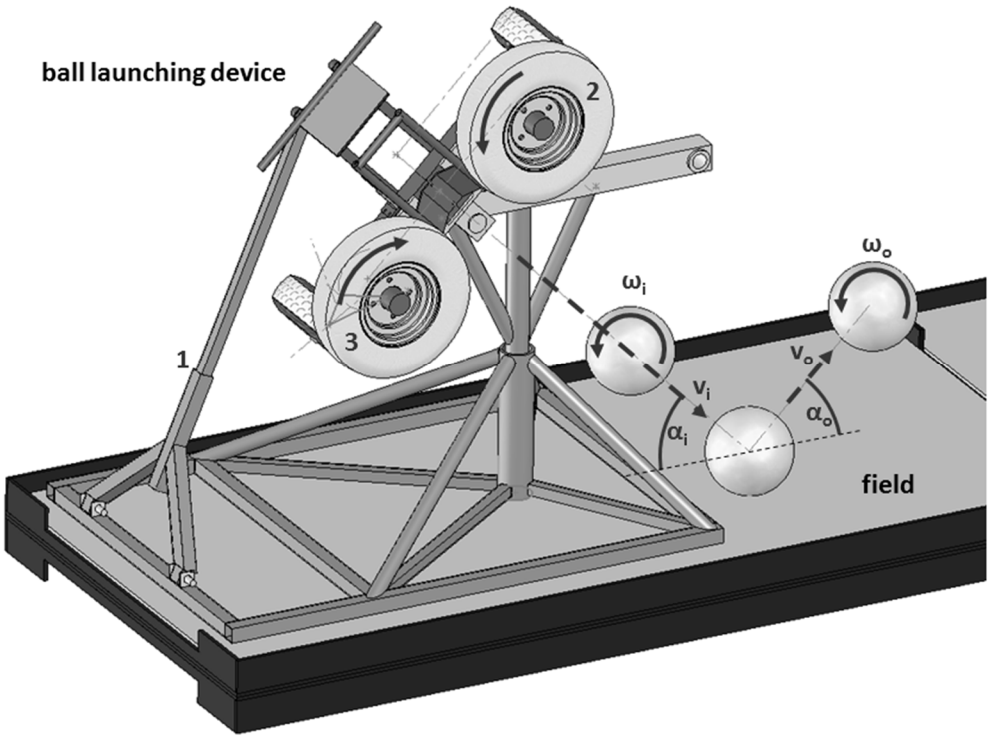

Figure 1: Test setup for oblique ball bounce.

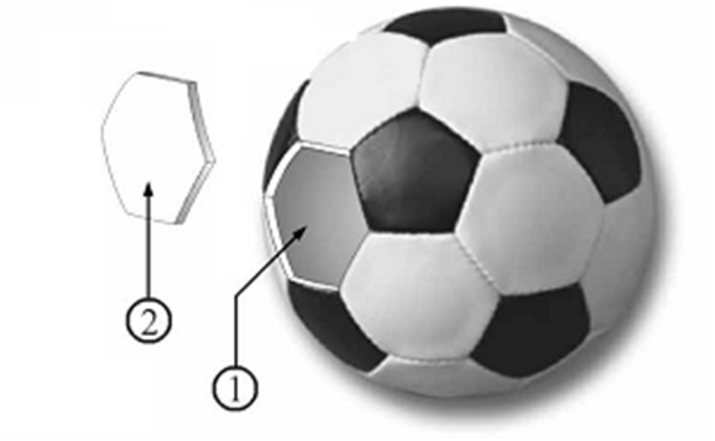

Figure 2: Soccer ball. 1: Internal Bladder. 2: Outer Panel.

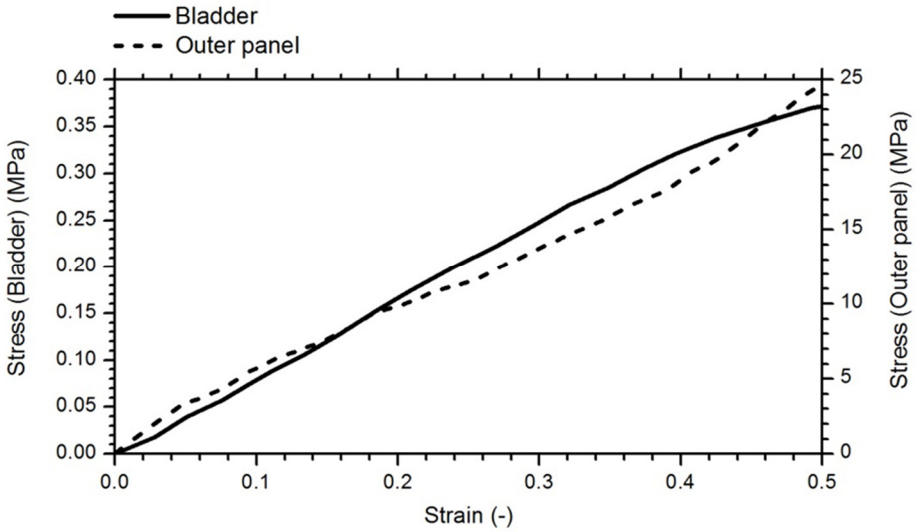

Figure 3: Stress-strain diagram of the bladder (Price, et al., 2006a).

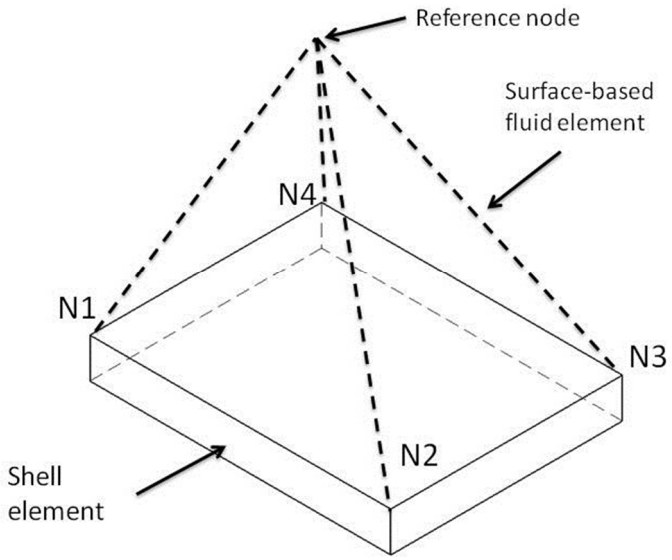

Figure 4: Arrangement of surface-based fluid element (Hydrostatic fluid element) and shell element.

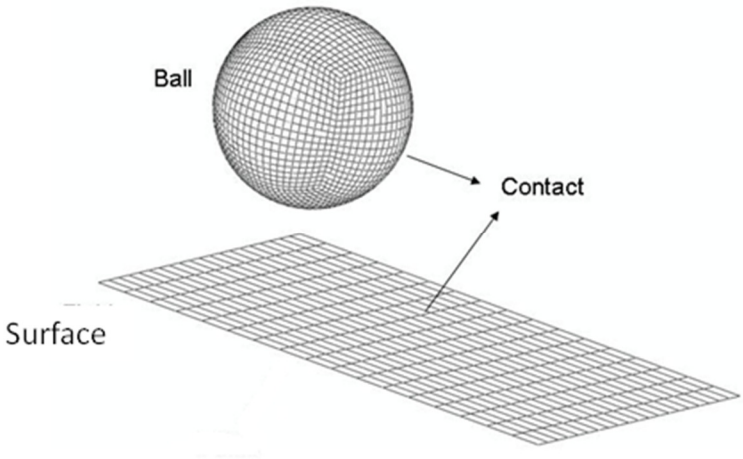

Figure 5: finite element model of the ball and surface.

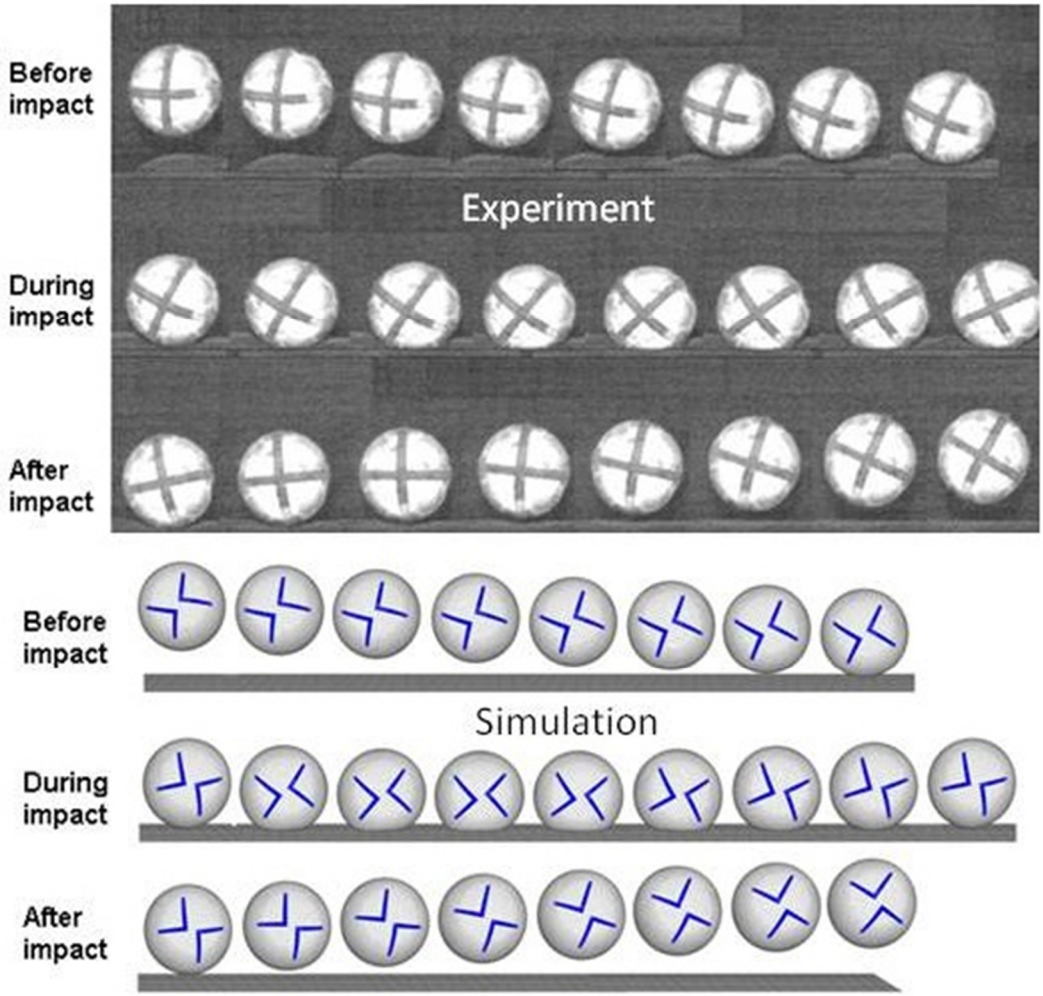

Figure 6: Comparison of high-speed camera images and simulation results of the oblique ball bounce for case *I*. Impact speed =19.05 m/s, Impact rotation = -59.66rad/s topspin, Impact angle = 29.60^{o}

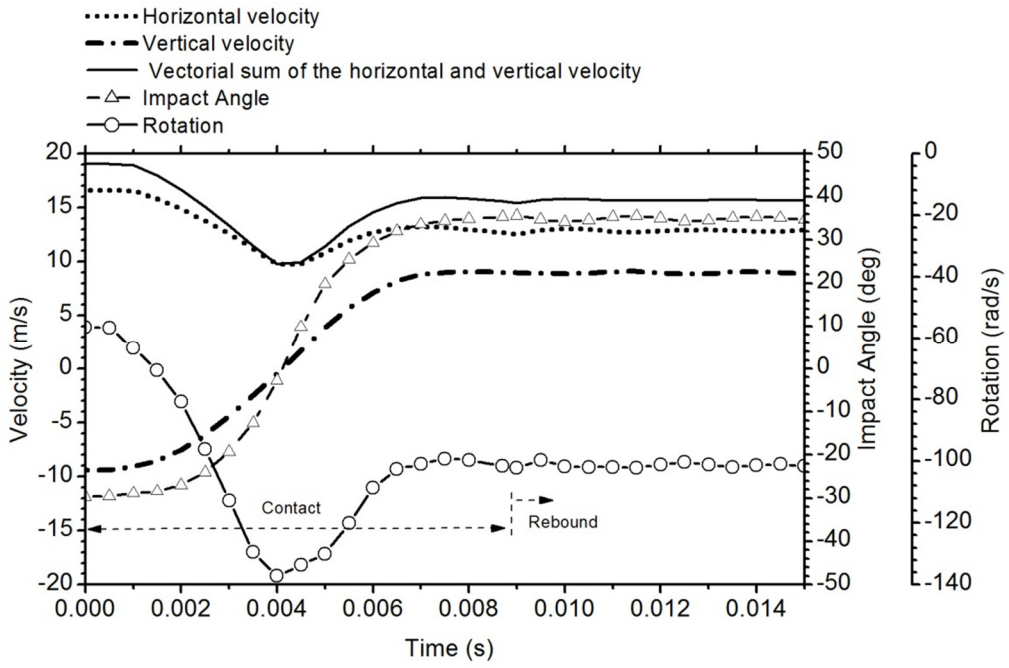

Figure 7: Simulation results for the speed, impact angle, and rotation of the ball during the impact for case *I*. Impact speed =19.05 m/s, Impact rotation = -59.66rad/s topspin, Impact angle = 29.60^{o}

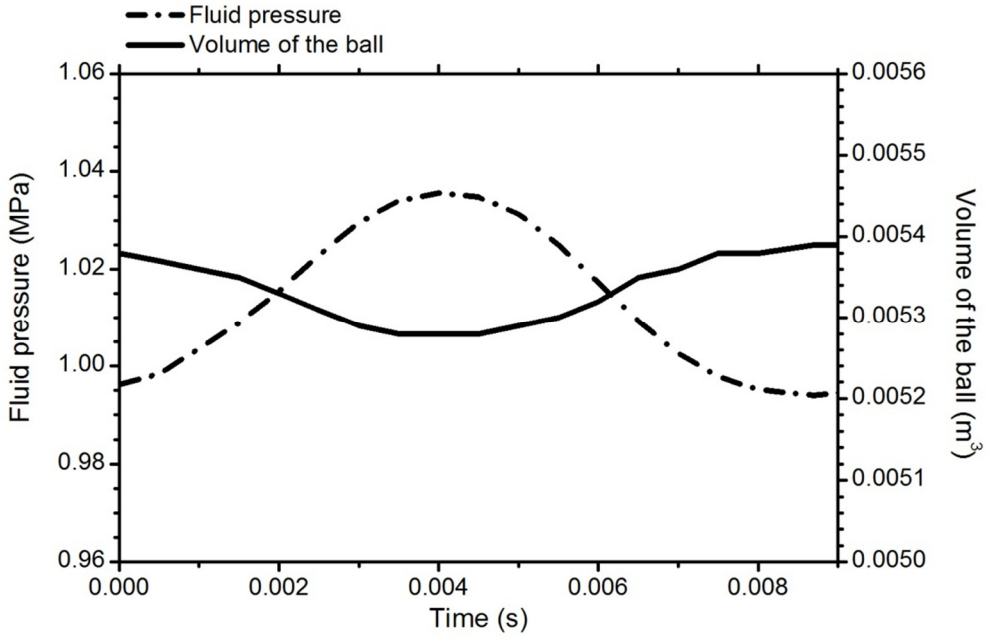

Figure 8: Simulation results for the air pressure and the ball volume during the impact for case *I*. Impact speed =19.05 m/s, Impact rotation = -59.66 rad/s topspin, Impact angle = 29.60^{o}

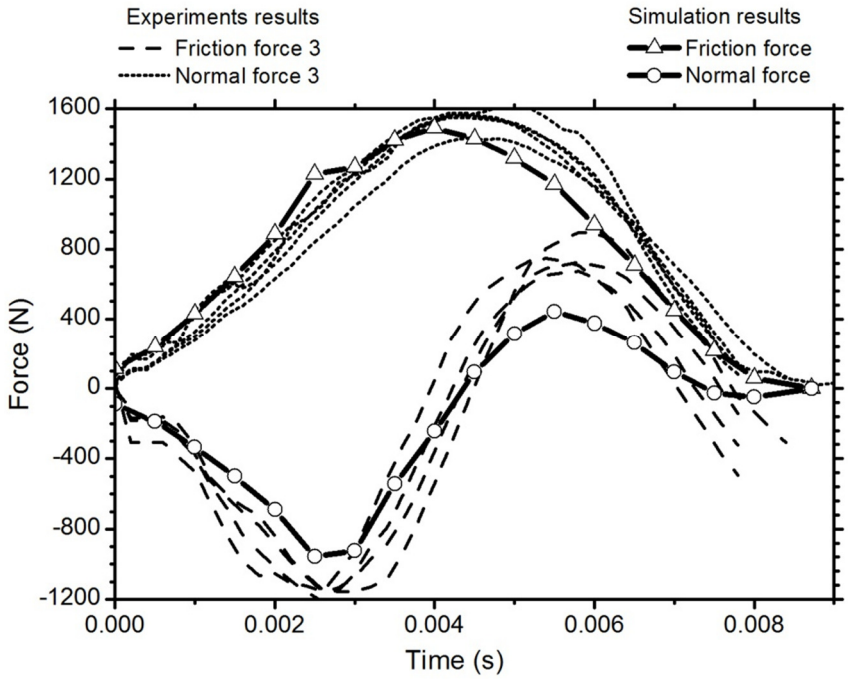

Figure 9: Comparison of the simulation and experimental results for the normal and friction force during the impact for case *I*. Impact speed =19.05 m/s, Impact rotation = -59.66 rad/s topspin, Impact angle = 29.60^{o}

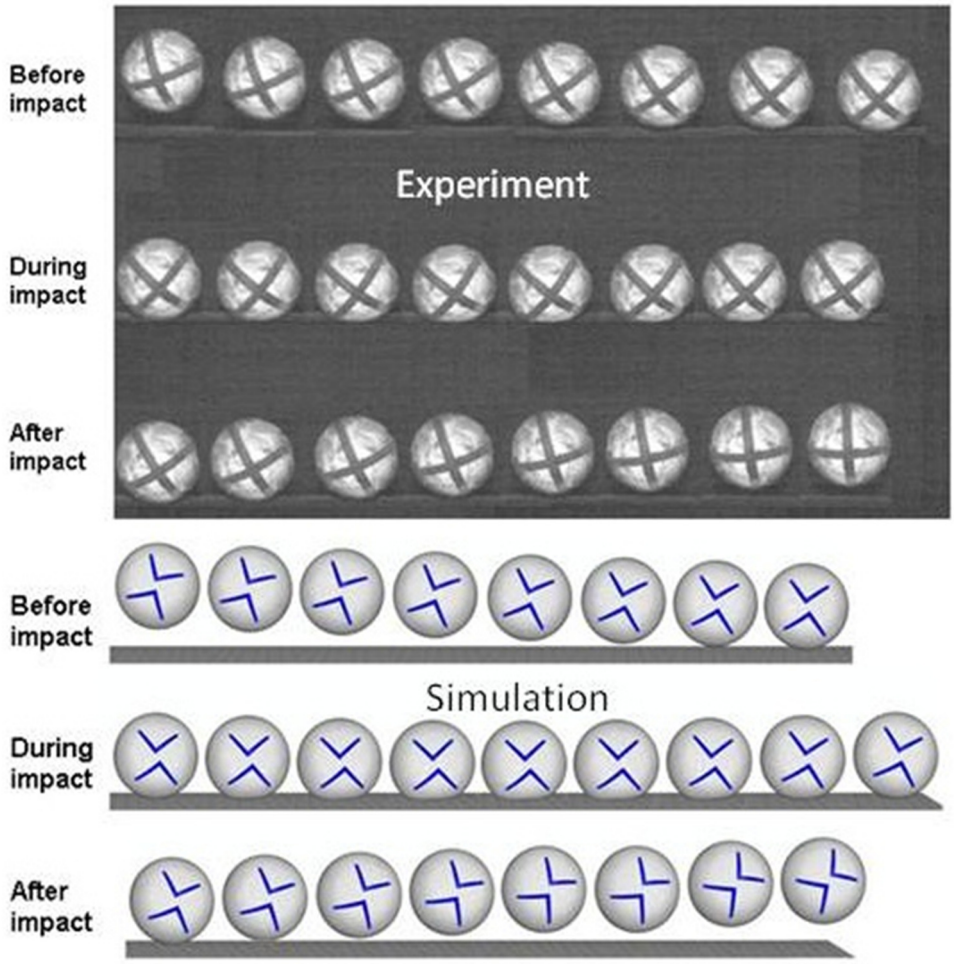

Figure 10: Comparison of high-speed camera images and simulation results of the oblique ball bounce for case *II*. Impact speed =18.08 m/s, Impact rotation = +58.40 rad/s backspin, Impact angle = 22.90^{o}

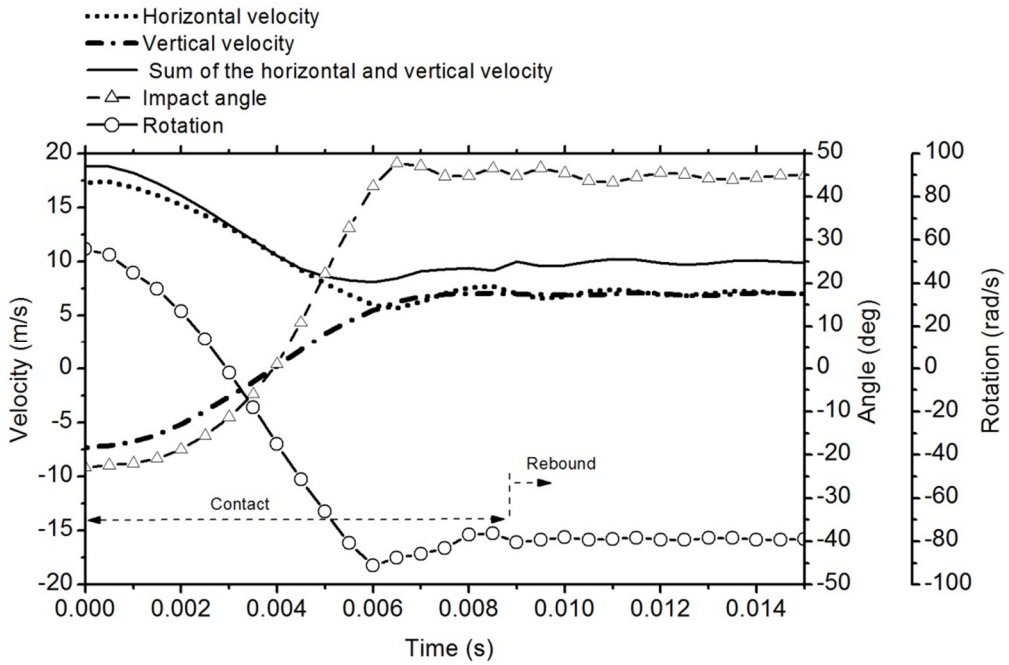

Figure 11: Simulation results for the speed, impact angle, and rotation of the ball during the impact for case *II*. Impact speed =18.08 m/s, Impact rotation = +58.40 rad/s backspin, Impact angle = 22.90^{o}

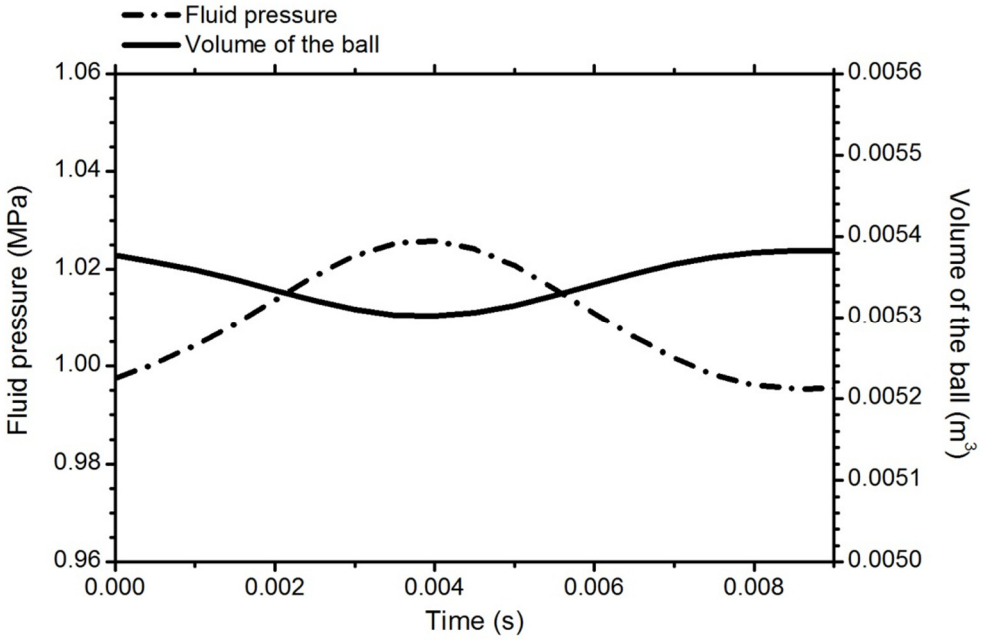

Figure 12: Simulation results for the air pressure and the ball volume during the impact for case *II*. Impact speed =18.08 m/s, Impact rotation = +58.40 rad/s backspin, Impact angle = 22.90^{o}

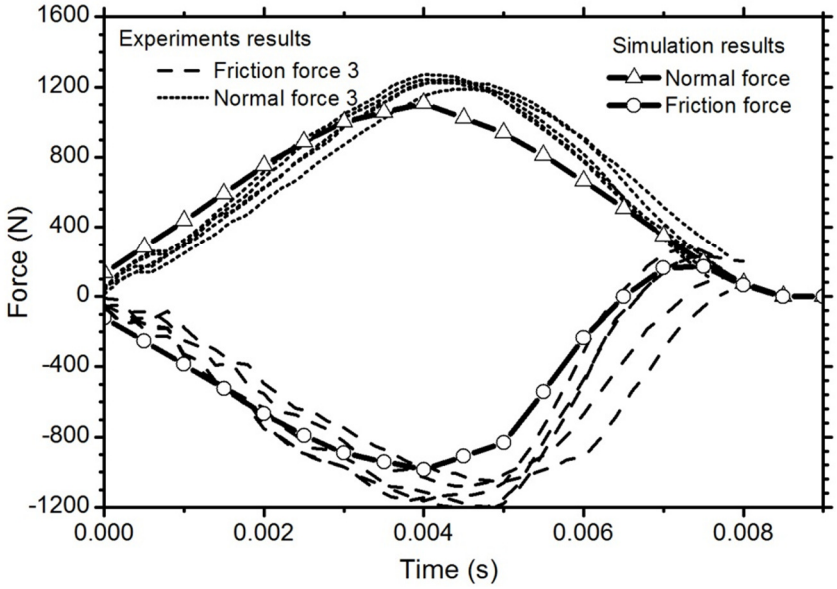

Figure 13: Comparison of the simulation and experimental results for the normal and friction force during the impact for case II. Impact speed =18.08 m/s, Impact rotation = +58.40 rad/s backspin, Impact angle = 22.90^{o}

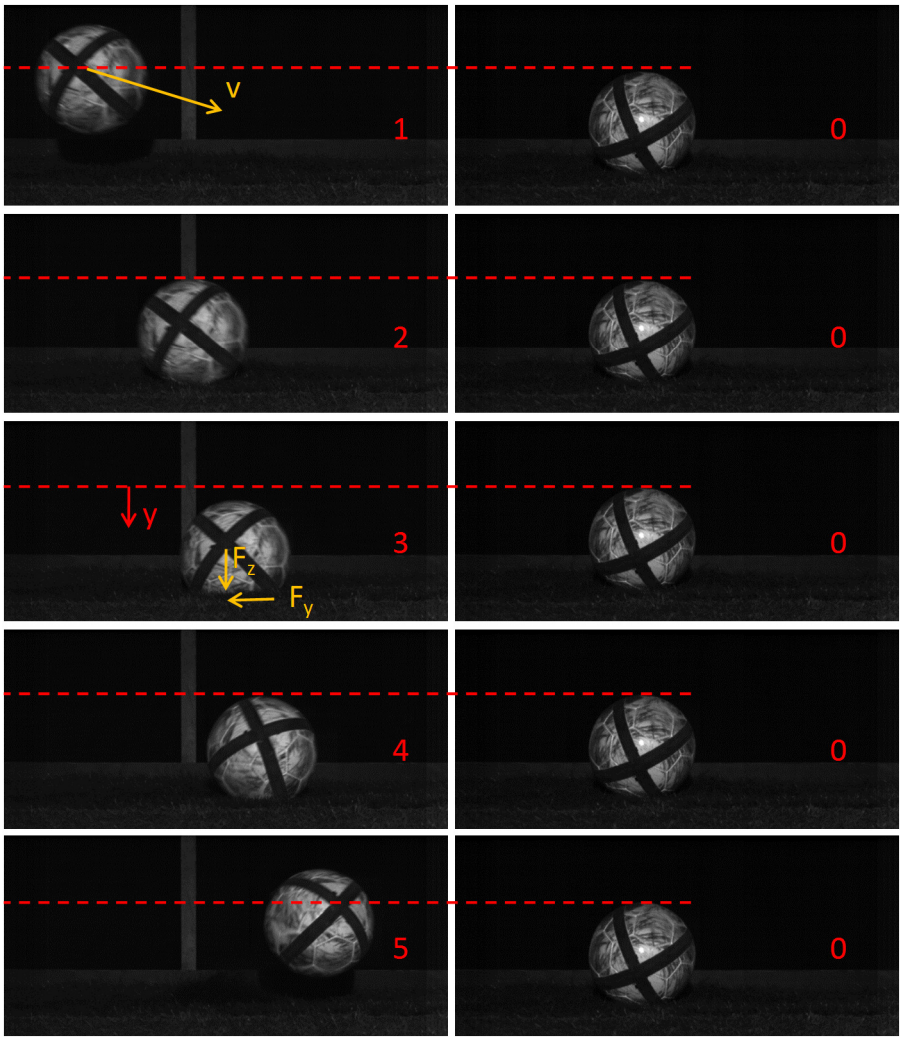

Figure 14: Close-up high speed images of oblique ball bounce for case *III* (0: neutral ball position, 1: before impact, 2: first ball contact, 3: maximum deformation, 4: ball leaves the ground, 5: after impact)

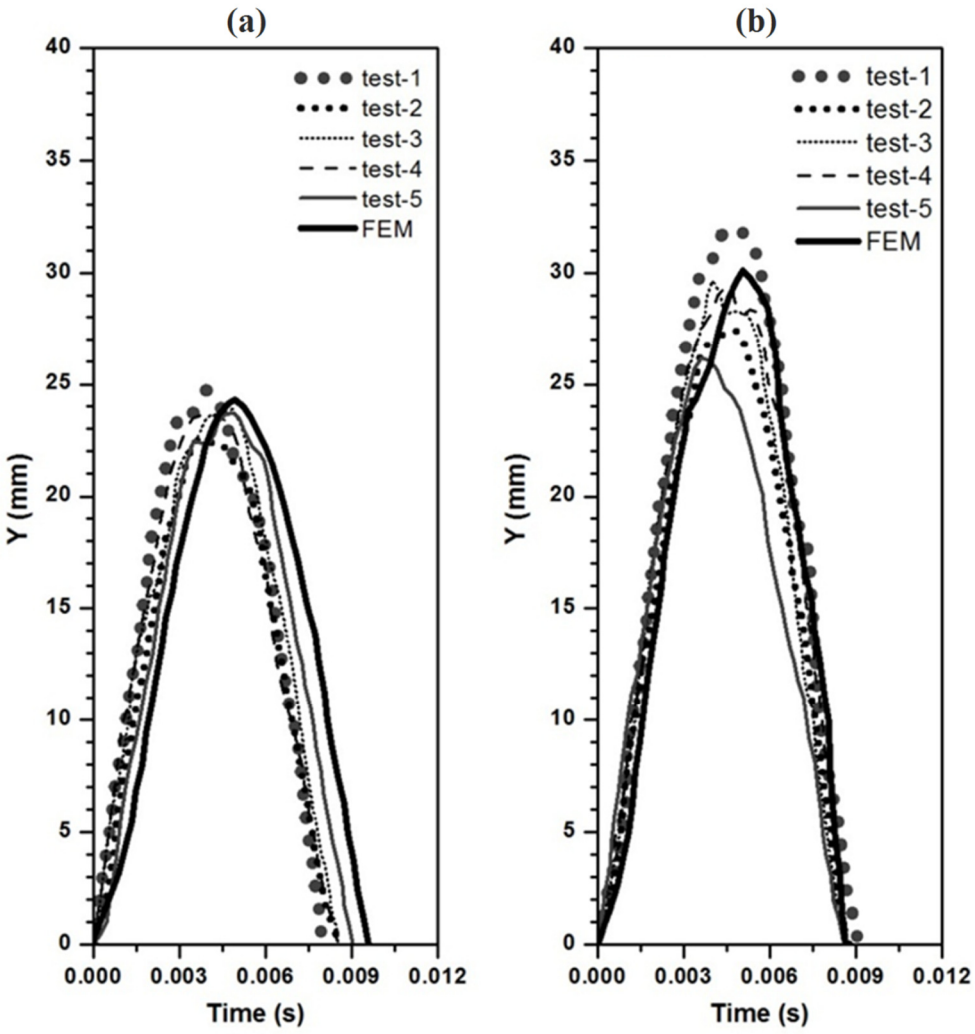

Figure 15: Comparison of measured and simulated ball deformation for case *III*. (a) Impact speed of 19.44 m/s (70 km/h); (b) Impact speed of 25.00 m/s (90 km/h))

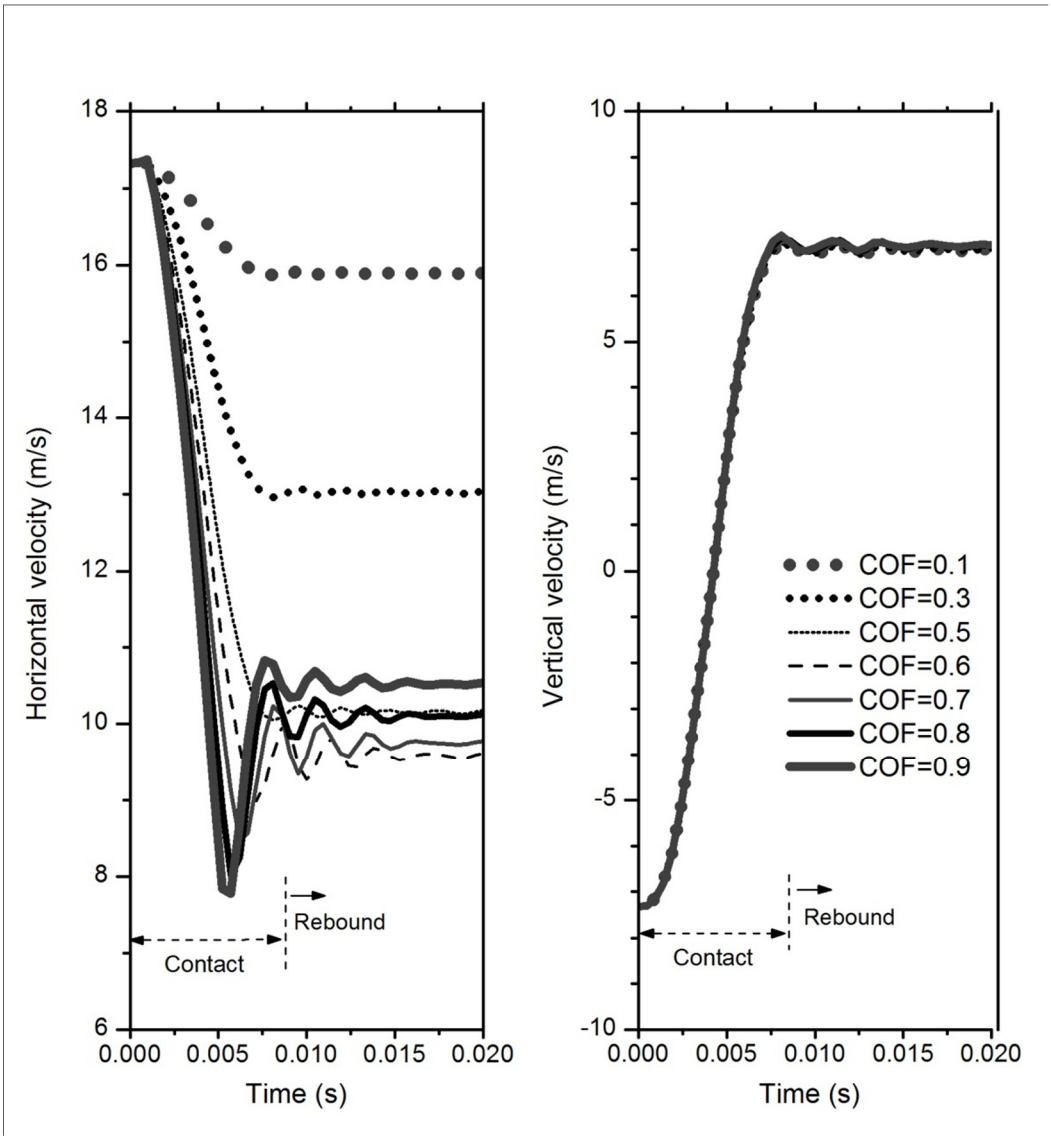

Figure 16: Effect of the friction coefficient on the horizontal and vertical speed of the ball.

Impact speed = 18.08 m/s, Impact rotation = 0 rad/s, Impact angle = 22.90^{o}

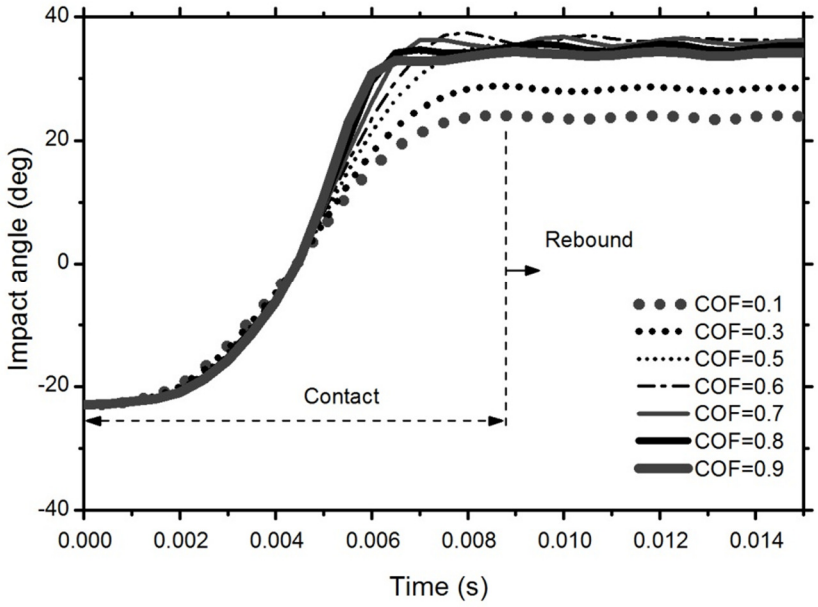

Figure 17: Effect of the friction coefficient on the bounce angle of the ball. Impact speed = 18.08 m/s, Impact rotation = 0 rad/s, Impact angle = 22.90^{o}

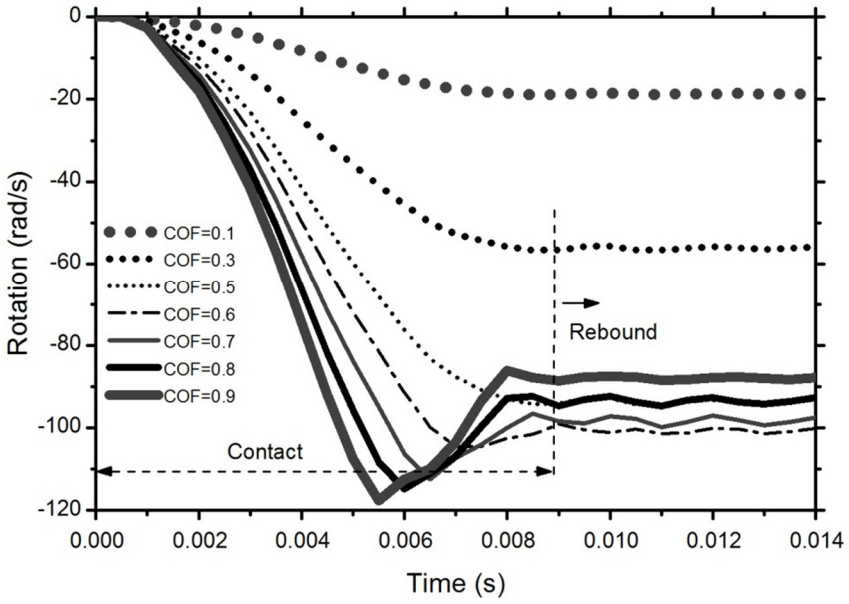

Figure 18: Effect of the friction coefficient on the rotational velocity of the ball. Impact speed = 18.08 m/s, Impact rotation = 0 rad/s, Impact angle = 22.90^{o}

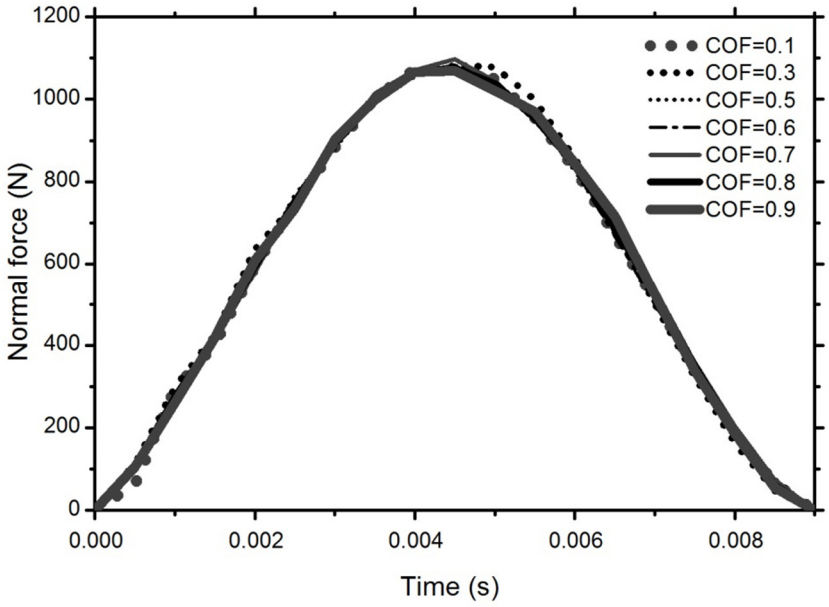

Figure 19: Effect of the friction coefficient on the normal force on the ball. Impact speed = 18.08 m/s, Impact rotation = 0 rad/s, Impact angle = 22.90^{o}

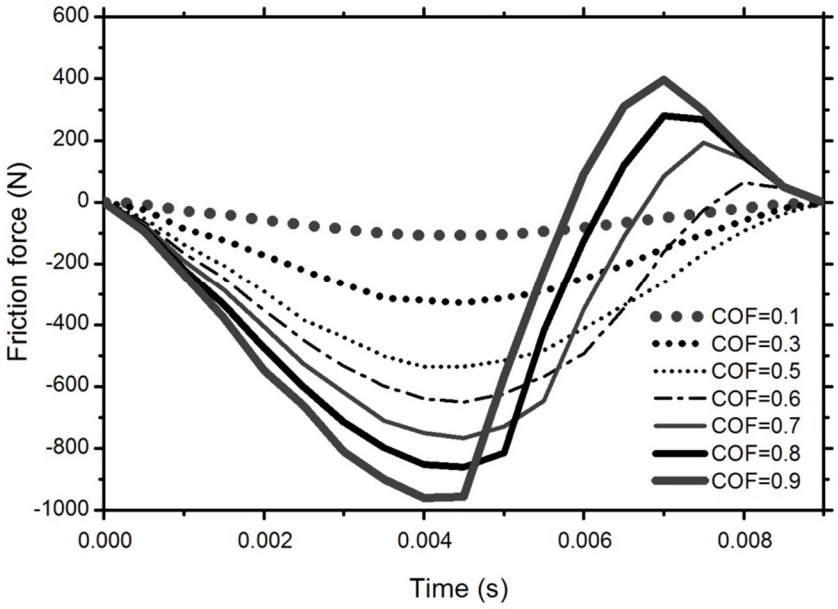

Figure 20: Effect of the friction coefficient on the friction force on the ball during the impact.

Impact speed = 18.08 m/s, Impact rotation = 0 rad/s, Impact angle = 22.90^{o}